Dedicated data analyses for improving PDFs :

Study of proton parton distribution functions at high x and charm production in charged DIS at HERA

(Phys. Rev. D 101 (2020) 112009 & JHEP 05 (2019) 201)

Ritu Aggarwal
SPPU, Pune, India

(on behalf of the ZEUS Collaboration)

Overview

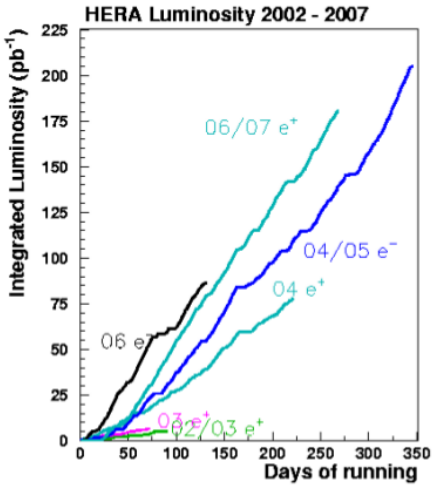

HERA upgrade

- Luminosity upgrade.
  - HERA I : 120 pb^{-1}
  - HERA II : 360 pb^{-1}

HERA-II

- *e* beam : 27.5 GeV
- *p* beam : 920 GeV
- Centre of mass E : 318 GeV
- H1 & ZEUS : General Purpose Detectors
- Data Taking : 1992-2007

- HERA-II upgrade (2002-2007):
  - Increased Luminosity
  - Polarized Lepton Beam
  - Improved Tracking system (MVD, STT)

Motivation of studying published high-x data

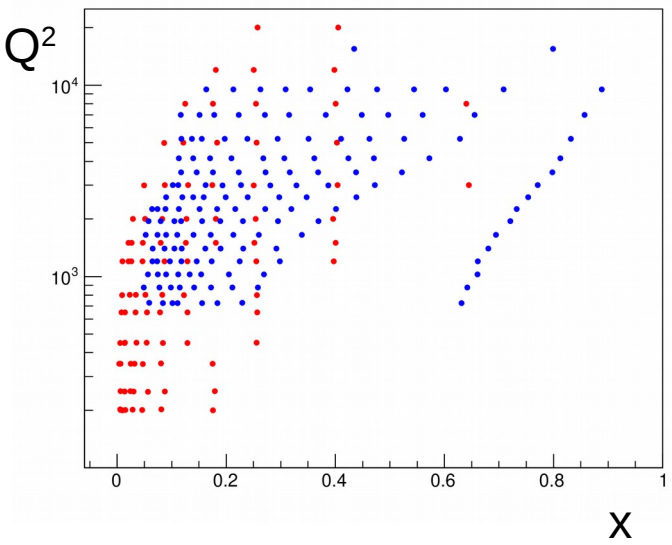

- high-Q^2 data
- high-x data

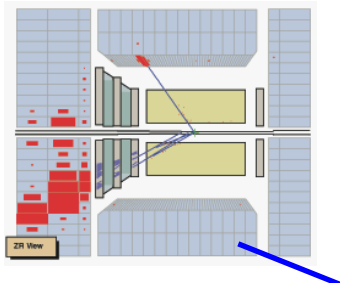

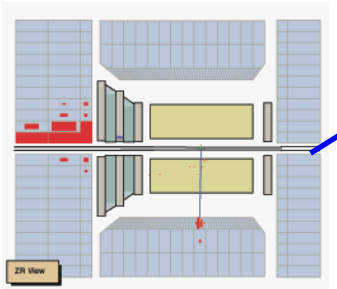

Integrated bins
(cross sections
Integrated in x)

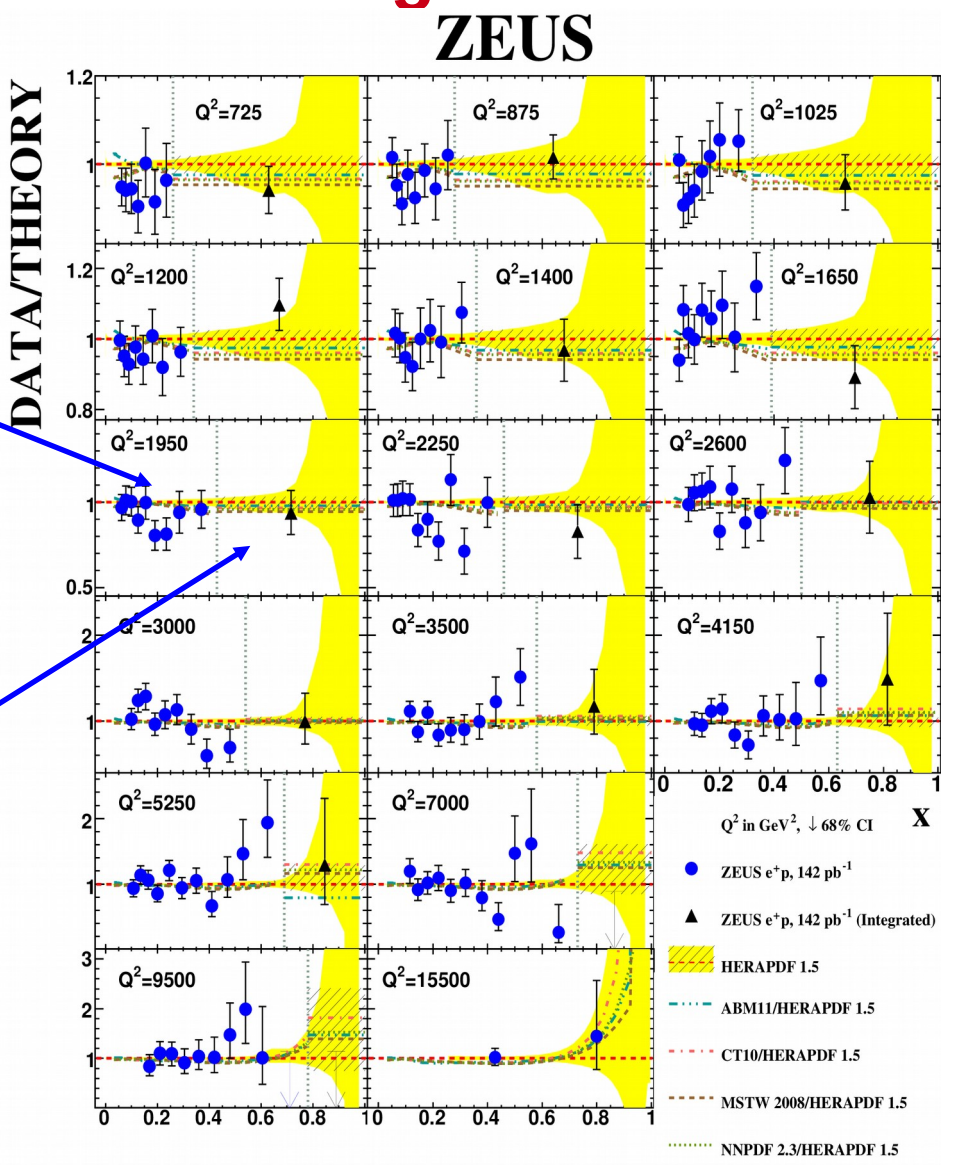

At present x upto 0.65 ZEUS data is included in PDF fits

Note the uncertainity bands above x ~ 0.65, can high-x data impact here

ZEUS Collaboration; H. Abramowicz et al. Measurement of Neutral Current e ± p Cross-Sections at High Bjorken x with the ZEUS Detector Phys. Rev. D 89 (2014) 072007

Technique to use high-x data

1) Some of the bins have low number of events / few have zero, poisson errors quoted.

2) Ofcourse it has a subset of data (high-Q^2 ZEUS data) already included in fits, but high-x data has more to say.

Transfer Matrix for the detector is developed using which number of events reconstructed in data can be predicted from any PDF ($\nu_{j,k}$) as below.

$$\nu_{j,k} = \mathcal{L} \int_{(\Delta x, \Delta Q^2)_j} \left[\int A(x_{\rm rec}, Q^2_{\rm rec} | x, Q^2) \times \frac{d^2\sigma(x, Q^2 | {\rm PDF}_k)}{dx dQ^2} dx dQ^2 \right] dx_{\rm rec} dQ^2_{\rm rec}.$$

$$\longrightarrow \quad \nu_{j,k} \approx \sum_i A_{ji} \lambda_{i,k}$$

$$\boldsymbol{\nu = T R \lambda}$$

$$T_{ji} = \frac{\sum_{m=1}^{M_i} \omega_m I(m \in j)}{\sum_{m=1}^{M_i} \omega_m^{\rm MC}}$$

$$R_{ii} = \frac{\sum_{m=1}^{M_i} \omega_m^{\rm MC}}{\mathcal{L}^{\rm MC} \sigma_{i,{\rm CTEQ5D}}}$$

L : data luminosity
R_{ii} : Radiative corrections (calculated using HERACLES)
$\lambda_{i,k}$: born level cross sections in i^{th} bin for k^{th} PDF

$\boldsymbol{T_{ji}}$: Transfer Matrix, has all detector and analysis effects
(probability of an event reconstructed in j^{th} bin to come from i^{th} true bin)

Transfer Matrix : Probability of an event reconstructed in j^{th} bin to come from i^{th} true bin

Tracing back the path of MC reconstructed events in the generated x-Q^2 phase space

$$T_{ji} = \frac{\sum_{n=1}^{M_i} \omega_n I(n \in j)}{\sum_{n=1}^{M_i} \omega_n^{MC}}$$

T_{ij} = probability of an event reconstructed in j^{th} bin to come from i^{th} bin

ω_m = MC weights given to m^{th} event in bin i

I = 1 if m^{th} event is reconstructed in bin j, else = 0

M_i = total events generated in i^{th} bin

$$\nu = T\,R\,\lambda$$

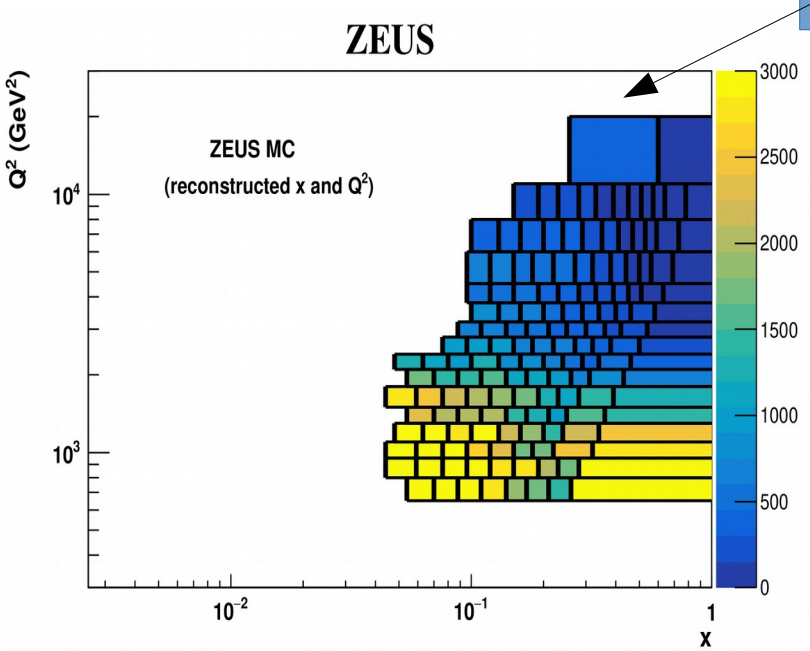

Reconstructed MC events in Cross section bins

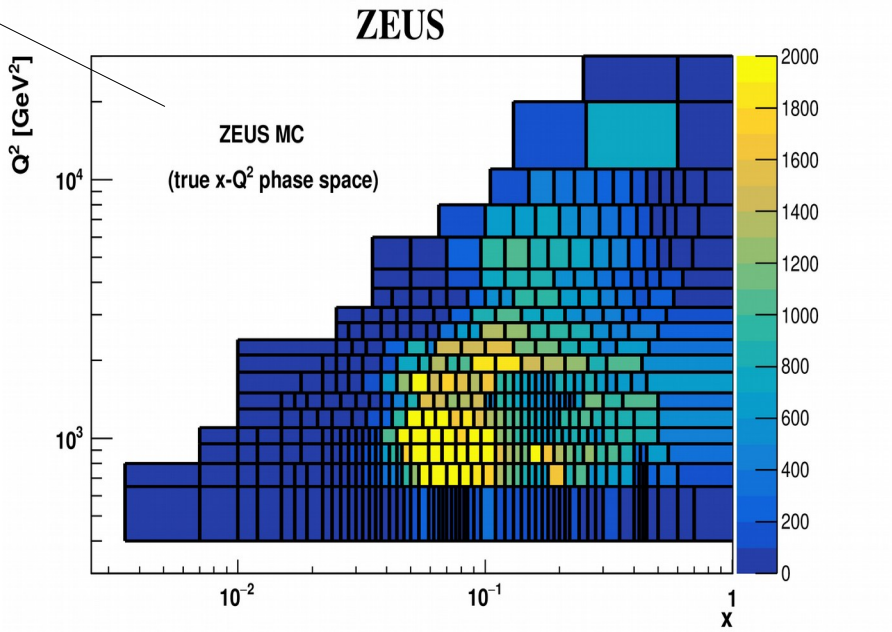

Generated distribution of these events

Comparison of Different PDFs

1) Comparison at generator level (μ = Rλ) from different PDFs.

2) Comparison at reconstructed level from different PDFs : Convolute μ with Transfer Matrix to get a prediction of number of events in the cross section b bins (ν) from different PDFs

- ν from different PDF is compared to observed events from data and Poisson statistics is used to probe how well given PDF is defining the data.

$$P(D|\mathrm{PDF_k}) = \prod_j \frac{e^{-\nu_{j,k}} \nu_{j,k}^{n_j}}{n_j!}$$

- Bayes factor, Δχ2 and p-value is determined for different PDFs

$$\Delta\chi^2_{k,l} = -2\ln\frac{P(D|\mathrm{PDF}_k)}{P(D|\mathrm{PDF}_l)}$$

- Comparison of p-values in high-x and lower-x range is shown for different PDFs

- Study of systematics uncertainties : Normalization uncertainty found significant (scales μ up and down)

Ratio of generator level cross sections in different PDFs to HERAPDF2.0NNLO (e+p)

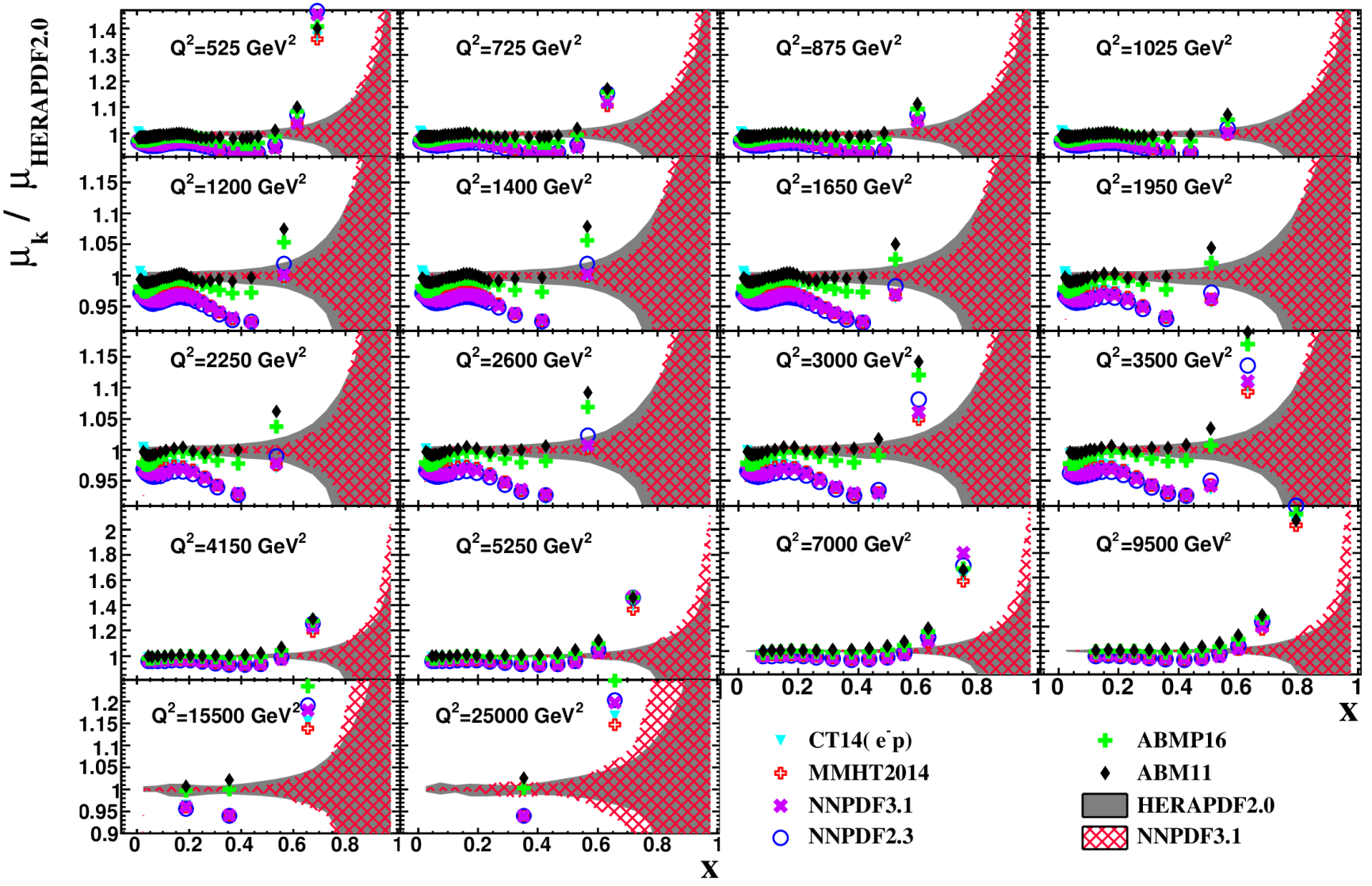

Probability of explaining high-x data from different PDFs

PDF	$e^- p$			$e^+ p$		
	p-value	P1/P2	$\Delta\chi^2$	p-value	P1/P2	$\Delta\chi^2$
HERAPDF2.0	2.8×10^{-2}	1.0	0.0	0.35	1.0	0.0
CT14	3.2×10^{-3}	7.6×10^{-3}	9.8	0.82	$5.9 \times 10^{+5}$	−27
MMHT2014	2.3×10^{-3}	2.1×10^{-3}	12	0.82	$4.7 \times 10^{+5}$	−26
NNPDF3.1	3.9×10^{-4}	3.2×10^{-6}	25	0.73	$9.0 \times 10^{+4}$	−23
NNPDF2.3	1.3×10^{-4}	2.3×10^{-7}	31	0.70	$4.2 \times 10^{+4}$	−21
ABMP16	2.6×10^{-2}	9.0×10^{-1}	0.21	0.64	$6.1 \times 10^{+2}$	−13
ABM11	3.3×10^{-2}	7.2×10^{-1}	0.67	0.45	2.8	−2.1

Conclusions :

- **p-values from MMHT2014, CT14nlo, NNPDF higher than HERAPDF2.0 for e^+p, much worse for e^-p**

PDF	$e^- p$				$e^+ p$			
	Lower x		Higher x		Lower x		Higher x	
	P1/P2	$\Delta\chi^2$	P1/P2	$\Delta\chi^2$	P1/P2	$\Delta\chi^2$	P1/P2	$\Delta\chi^2$
HERAPDF2.0	1.0	0.0	1.0	0.0	1.0	0.0	1.0	0.0
CT14	6.0×10^{-1}	1.0	1.3×10^{-2}	8.7	$1.6 \times 10^{+3}$	−15	$3.6 \times 10^{+2}$	−12
MMHT2014	7.1×10^{-2}	5.3	2.9×10^{-2}	7.1	$1.3 \times 10^{+3}$	−14	$3.7 \times 10^{+2}$	−12
NNPDF3.1	9.1×10^{-5}	19	3.5×10^{-2}	6.7	$2.5 \times 10^{+2}$	−11	$3.6 \times 10^{+2}$	−12
NNPDF2.3	8.0×10^{-6}	23	2.9×10^{-2}	7.1	$1.2 \times 10^{+2}$	−9.5	$3.7 \times 10^{+2}$	−12
ABMP16	2.3×10^{-1}	3.0	4.0	−2.7	$4.8 \times 10^{+1}$	−7.8	$1.3 \times 10^{+1}$	−5.1
ABM11	2.3×10^{-1}	3.0	3.2	−2.3	4.2	−2.9	6.7×10^{-1}	0.8

F. Beaujean et al, p-values for model evaluation, Phys. Rev. D 83, 012004 (2011). arXiv:1011.1674

Charm Production in CC DIS at HERA

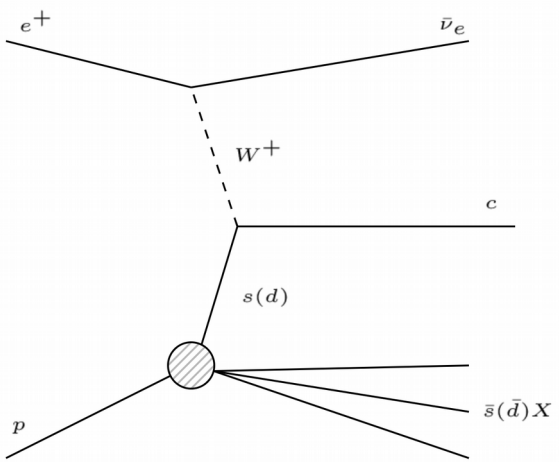

(i)

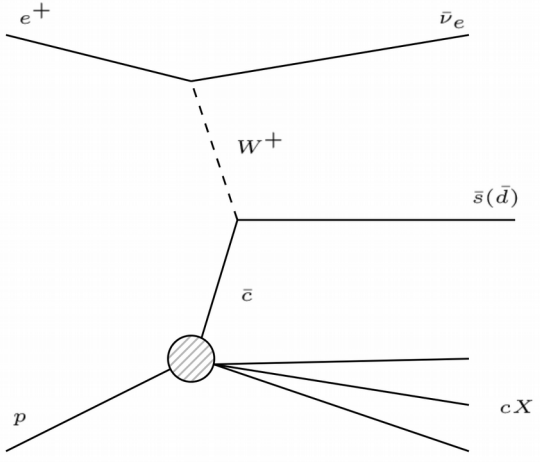

(ii)

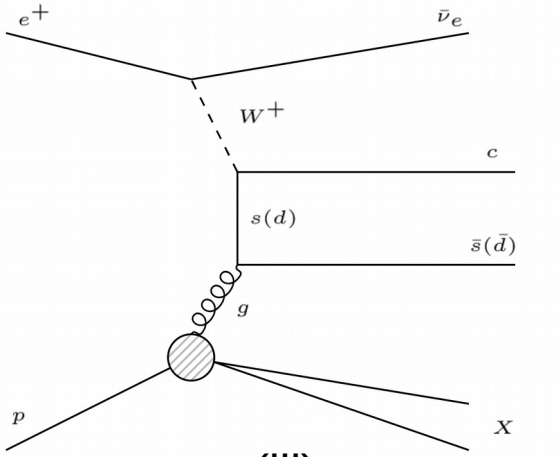

(iii)

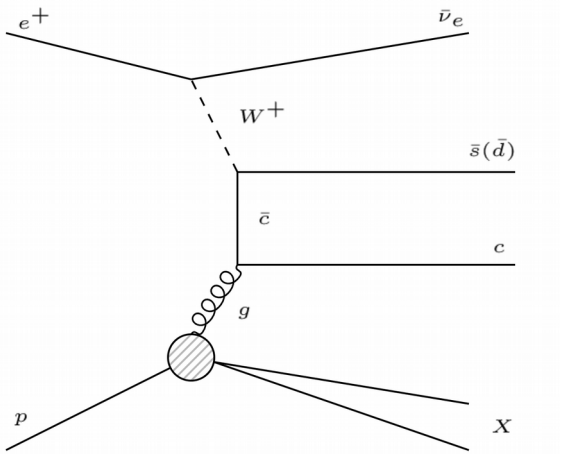

(iv)

- Charm production processes in e^+p CCDIS

QPM-like
- *i.* $s\bar{s}(d\bar{d})W^+ \rightarrow c\bar{s}(\bar{d})$
- *ii.* $c\bar{c}W^+ \rightarrow c\bar{s}(\bar{d})$

BGF-like
- *iii.* $g \rightarrow s\bar{s}(d\bar{d})$
- *iv.* $g \rightarrow c\bar{c}$

- Subprocess (i) is directly sensitive to the strangeness of the proton.

- However, these subprocesses are distinguishable only in the QCD scheme.

  → Extraction of $s(x, Q^2)$ is model dependent.

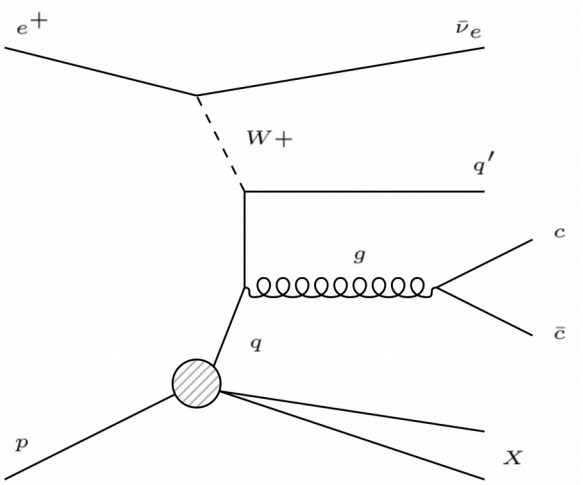

QCD part

Strangeness in proton (model dependent)

- Mass-suppressed strangeness : $f_s \left(\equiv \frac{s}{s+\bar{d}}\right) \sim 0.3$
  - For large x_{Bj}, experimentally supported by neutrino-scattering experiments (CCFR/NuTeV, NOMAD, CHORUS).
- Unsuppressed strangeness : $f_s \sim 0.5$
  - For small x_{Bj}, experimentally supported by high-precision W/Z production measurement (ATLAS) & $W + c$ data (CMS).
- x-dependent strangeness
  - As suggested by HERMES
  - $x\bar{s} = f_s' \; 0.5 \tanh\left(-20 \; (x - 0.07)\right) x\bar{D}$

Theory Predictions :

=> ***Zero-mass variable-flavour-number scheme***

(QCDNUM, HERAPDF2.0, ATLAS epWZ16 PDF)

Used for relative comparison of different assumptions on strange content

=> ***Fixed-flavour number scheme (FFN)***

No charm content & larger gluon content

=> ***General mass VFNS scheme(GM-VFNS)***

FONLL-B scheme used for comparisons

CC DIS Kinematic variables reconstruction

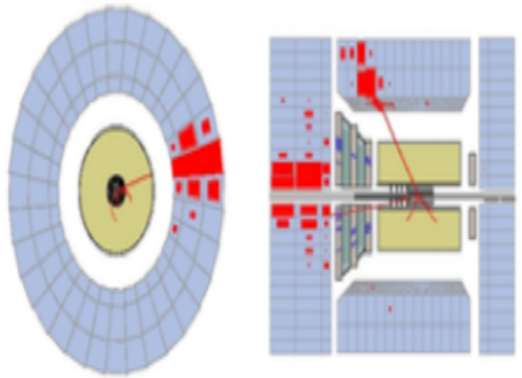

Jacquet Blondel Variables used due to missing final state lepton information

$$y_{JB} = \frac{\sum_h (E - p_z)_h}{2E_e},$$

$$Q^2_{JB} = \frac{p^2_{T,h}}{1 - y_{JB}},$$

$$x_{JB} = \frac{Q^2_{JB}}{s y_{JB}}.$$

- Kinematic selection cut
  - $200 < Q^2 < 60000\ GeV^2$
  - $y < 0.9$

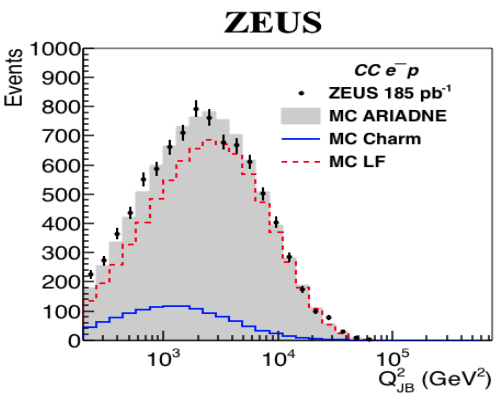

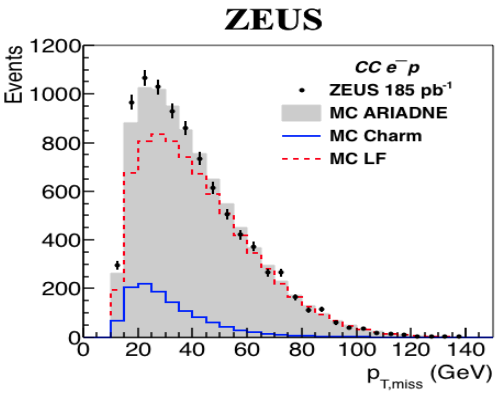

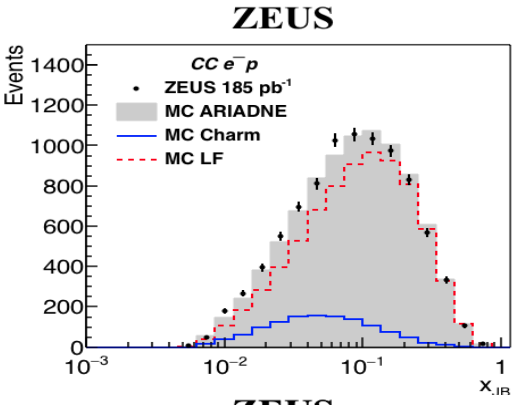

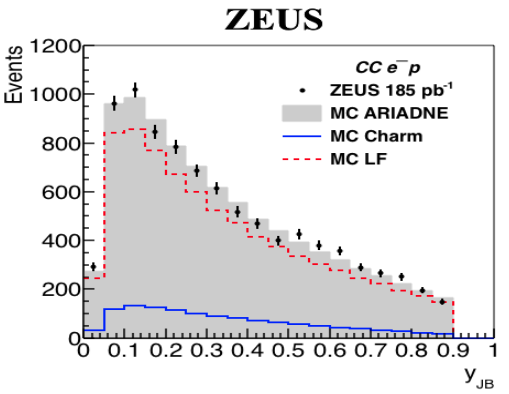

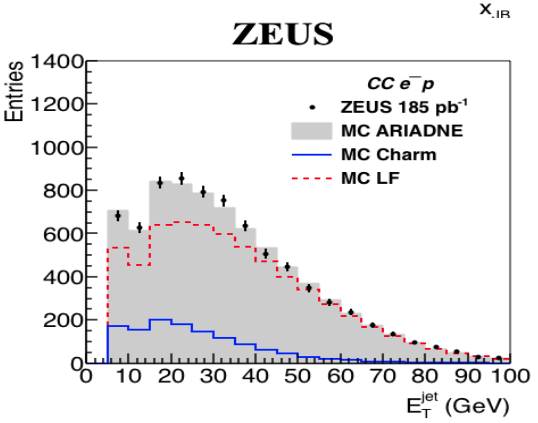

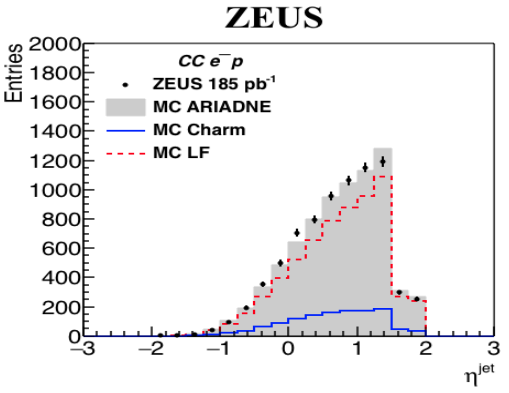

Charm Tagging

Charm identification

Lifetime-tagging Method

- 2D decay length (L_{xy}) projected onto Jet axis.
  - LF → Prompt, Symmetric decay length dist.
  - Charm → Weakly-decaying, Asymmetric dist.
- LF contribution (background) suppressed by mirroring decay length distribution about $L_{xy} = 0$.
  $(L_+ - L_-, S_+ - S_-)$

*S = significance

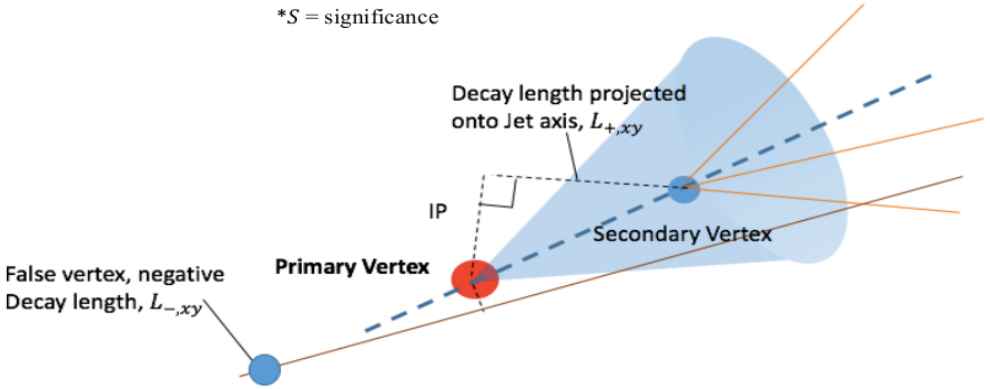

- Asymmetric charm distribution observed.
- Significance cut, $S > 2$, to improve statistical uncertainty.

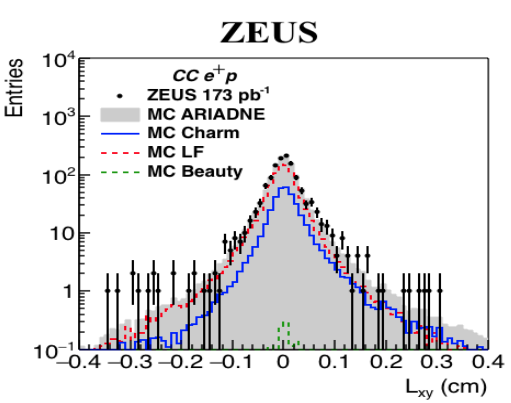

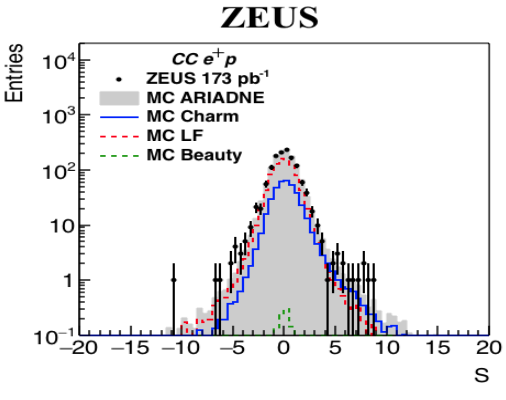

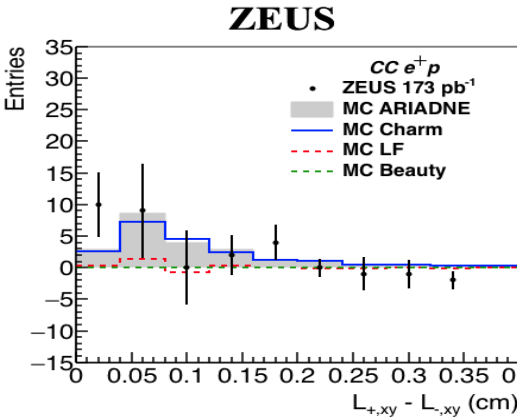

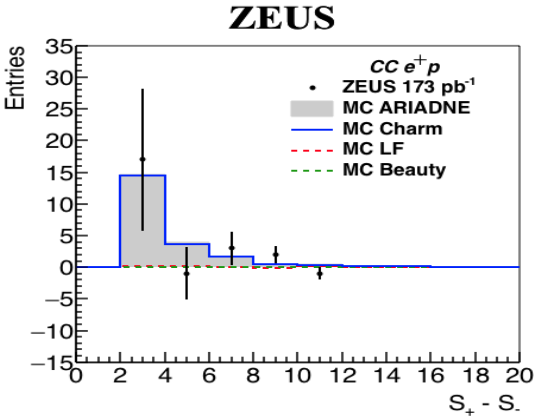

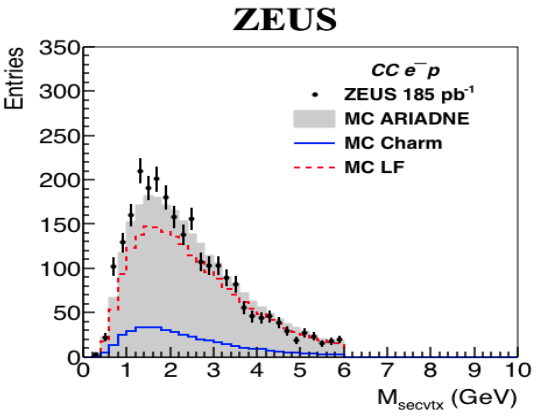

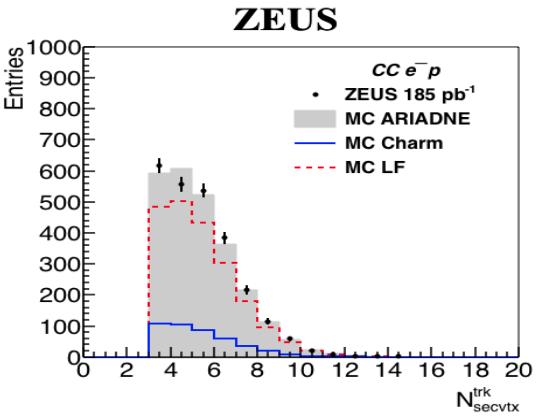

Results

- Visible charm cross section

$$\sigma_{c,vis} = \frac{N^{data} - N_{bg}^{MC}}{N_c^{MC}} * \sigma_c^{MC} = \frac{N^{data} - N_{bg}^{MC}}{N_c^{MC}} * \frac{N_{vis}}{L}$$

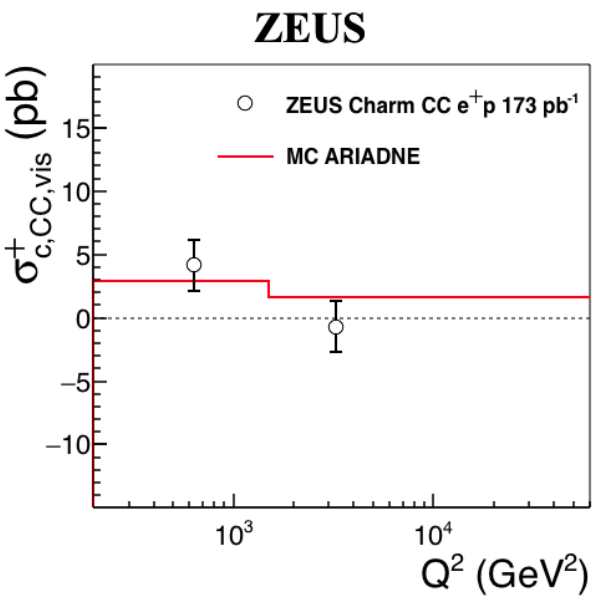

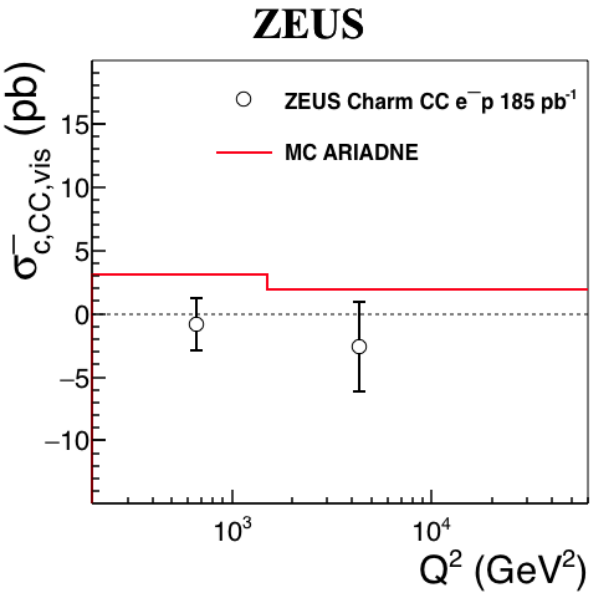

- EW charm cross section is extrapolated via $C_{ext} = N_{full}^{EW}/N_{vis}^{EW}$

$$\sigma_{c^{EW}} = C_{ext}\sigma_{c^{EW},vis}$$

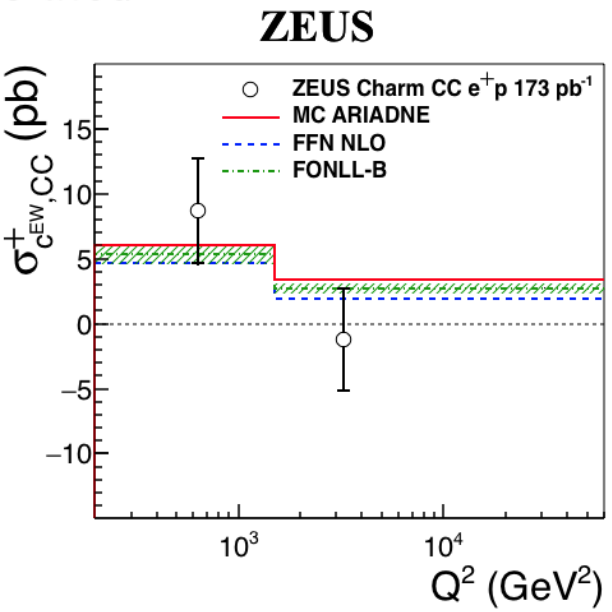

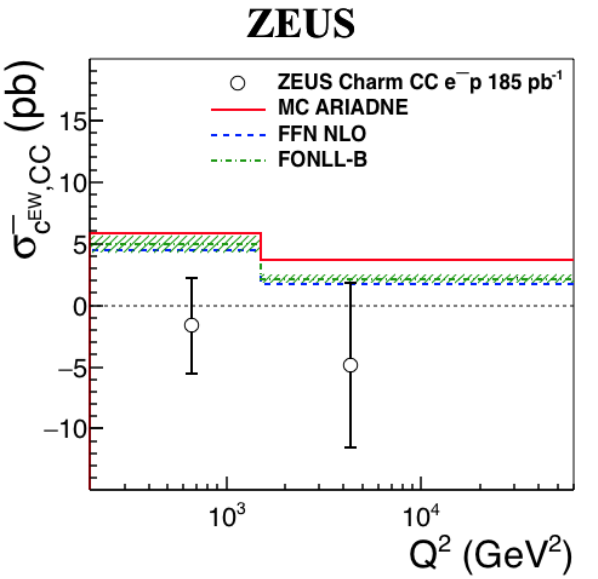

Conclusions – I (NC DIS high-x analysis at ZEUS)

Technique of building Transfer Matrix for high-x ZEUS data Shown.

--Transfer Matrix can be used to predict number of events in the given cross section bins in MC.

-- Transfer Matrix can be used to compare number of events predicted by different PDFs.

Bayes factor, p-values from different PDFs calculated and shown on the basis of their explanation to the high-x data using Transfer Matrix.

-- Differences are seen between different PDFs
-- Differences are also there for e-p and e+p data sets and the higher and lower x ranges.

p-values from dominant systematic uncertainty of normalization error shown.

Direction on how to include high-x data in PDF fits provided.

Conclusions – II (Charm CC DIS analysis at ZEUS)

EW charm production measured for the first time in high-Q^2 CC DIS ep at HERA

--Consistent with theory

-- Though statistically limited

-- More statistics needed to investigate the strangeness in proton

-- Possible at future detectors with high luminosity and better vertex detecting techniques

-- and with some improvement in theory calculations

-- better understanding of strangeness in future colliders expected.

Thanks !

Back up

Nomalization Error : Vary generated events by 1.8 % up and down and calculate new p-value

	e^-p				e^+p			
	Lower x		Higher x		Lower x		Higher x	
PDF	P1/P2	$\Delta\chi^2$	P1/P2	$\Delta\chi^2$	P1/P2	$\Delta\chi^2$	P1/P2	$\Delta\chi^2$
				+1.8%				
HERAPDF2.0	1.7×10^{-3}	13	0.08	5.0	8.6×10^{-5}	19	0.01	9.8
CT14	28	−6.7	16	−5.5	5.0×10^{-2}	6.0	0.37	2.0
MMHT2014	$1.1 \times 10^{+2}$	−9.5	13	−5.1	0.11	4.4	0.31	2.3
NNPDF3.1	$4.9 \times 10^{+3}$	−17	15	−5.4	2.2	−1.5	0.36	2.0
NNPDF2.3	$1.8 \times 10^{+4}$	−20	18	−5.8	5.9	−3.6	0.41	1.8
ABMP16	0.37	2.0	0.30	2.4	2.6×10^{-3}	12	0.02	7.8
ABM11	9.6×10^{-3}	9.3	0.07	5.3	2.9×10^{-4}	16	0.01	10
				−1.8%				
HERAPDF2.0	0.69	0.74	1.7	−1.1	93	−9.1	30	−6.8
CT14	4.9×10^{-5}	20	9.3×10^{-3}	9.3	0.18	3.4	0.66	0.83
MMHT2014	1.2×10^{-5}	23	1.1×10^{-2}	8.9	8.0×10^{-2}	5.0	0.77	0.51
NNPDF3.1	3.1×10^{-7}	30	9.8×10^{-3}	9.3	4.4×10^{-3}	11	0.67	0.79
NNPDF2.3	8.5×10^{-8}	33	8.2×10^{-3}	9.6	1.6×10^{-3}	13	0.59	1.1
ABMP16	3.5×10^{-3}	11	0.46	1.5	3.3	−2.4	12	−4.9
ABM11	0.12	4.2	1.9	−1.3	28	−6.6	33	−7.0

Conclusions : Dominant systematics : due to error in normalization of data quoted as 1.8 %

- **p-values from different PDFs change differently**
- **Similar behavior as when using only statistical fluctuations.**

TABLE VI. List of $e^{\pm}p$ combined data points [9] to be removed and the ZEUS high-x data points [8] to be added. See Sec. VI for details.

HERA combined points to be removed	
x	Q^2 (GeV^2)
0.4	1200 1500 2000 3000 20000
0.6	3000 8000

ZEUS high-x data to be added	
x	Q^2 (GeV^2)
Integrated	725 875 1025 1200 1400 1650 1950 2250 2600 3000 3500 4150 5250 7000 9500
0.37	1950
0.4	2250
0.35, 0.44	2600
0.39, 0.48	3000
0.57	4150
0.53, 0.62	5250
0.56, 0.66	7000
0.54, 0.61, 0.71	9500
0.8	15500

Average ratio of Born level cross sections in different PDFs to HERAPDF2.0NNLO for M bins (e-p)

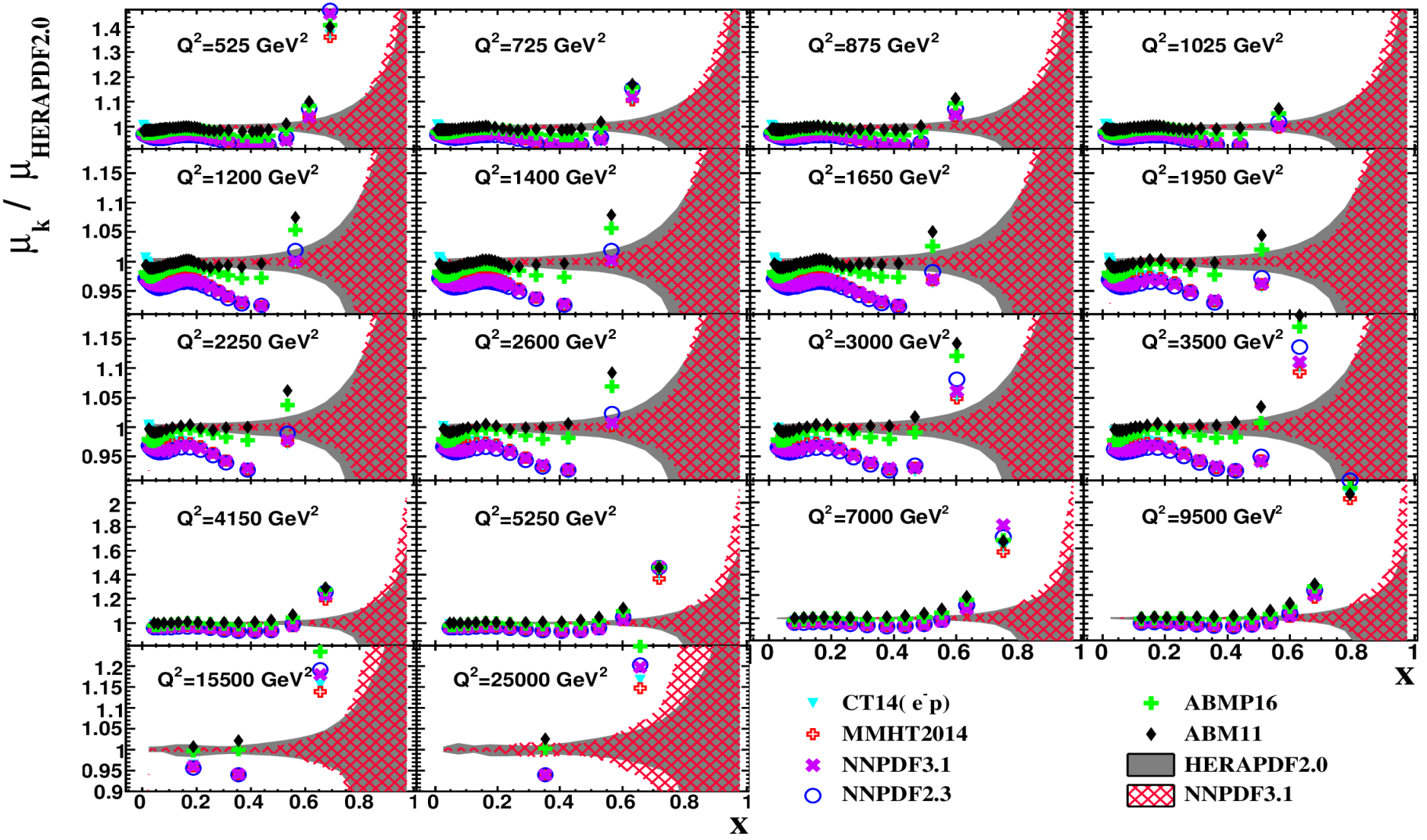

Ratio of No. of events in data to HERAPDF2.0 NLO and 1,2,3 sigma bands from Poisson Statistics

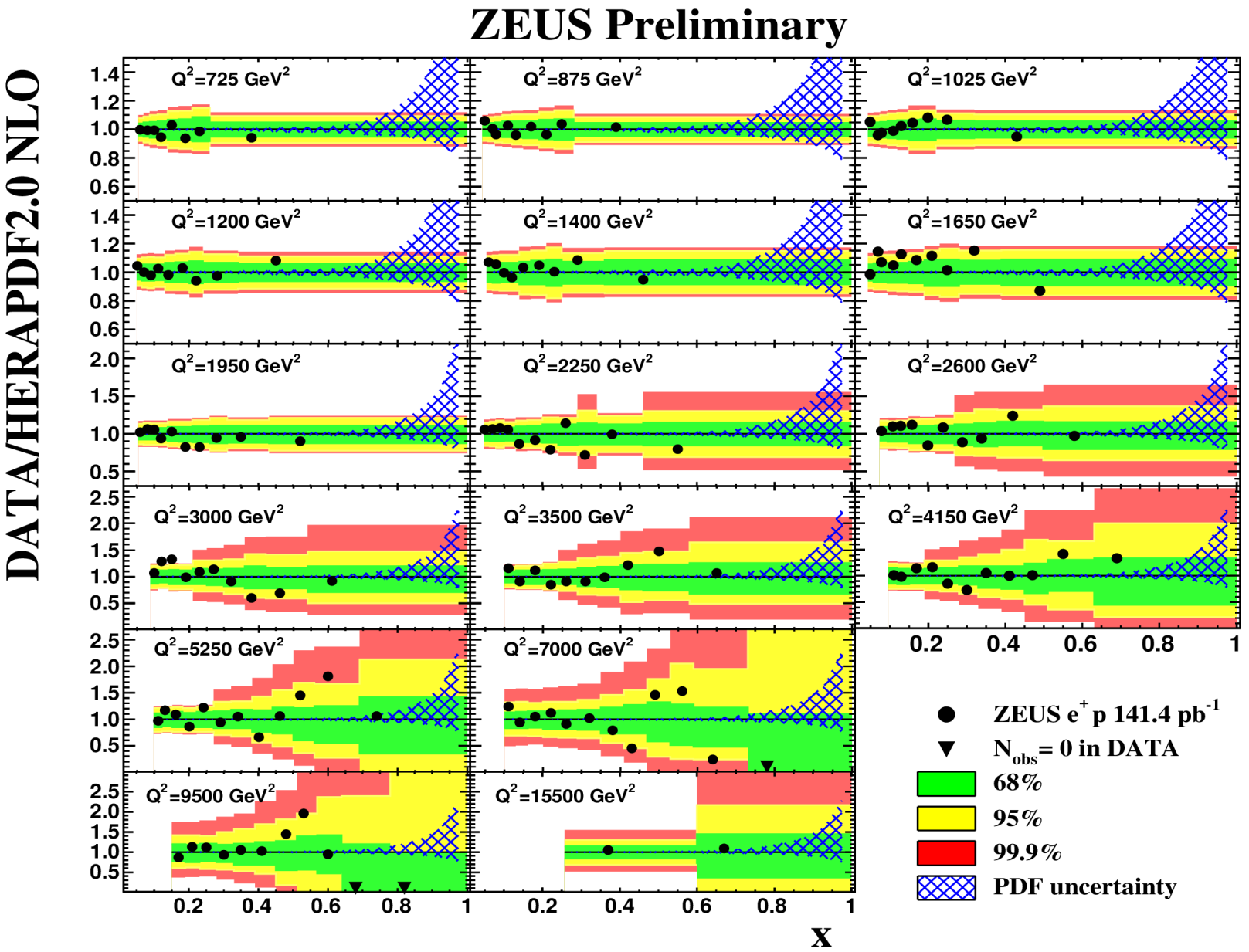

R. Aggarwal, A. Caldwell, Error bars for distributions of numbers of events. Eur. Phys. J. Plus 2012, 127, 1–8.

Ratio of No. of events in data to HERAPDF2.0 NLO and 1,2,3 sigma bands from Poisson Statistics

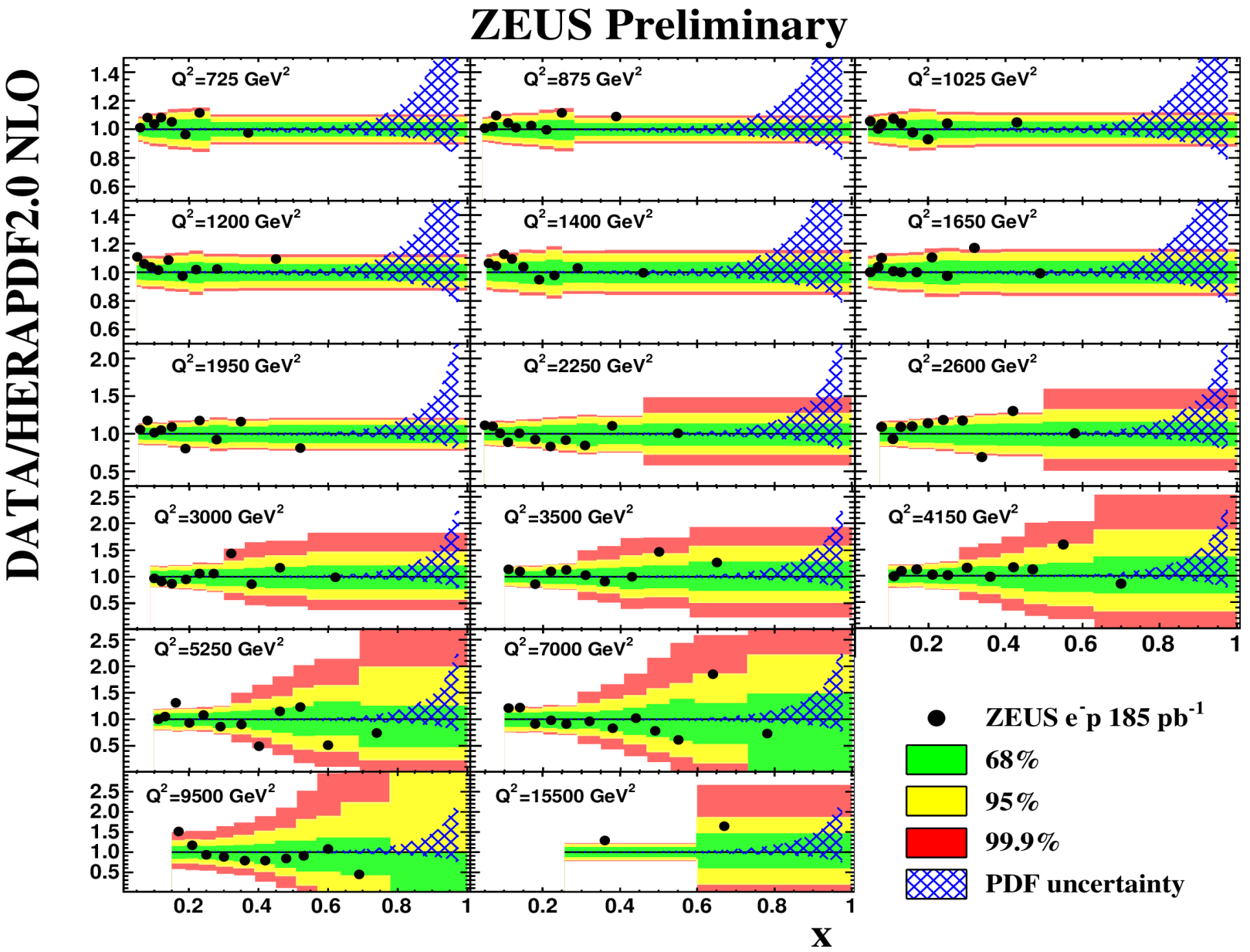

P-value determination

Total probability for each PDF :

$$P(D|M_k) = \prod_j \frac{e^{-\nu_{j,k}} \nu_{j,k}^{n_j}}{n_j!}$$

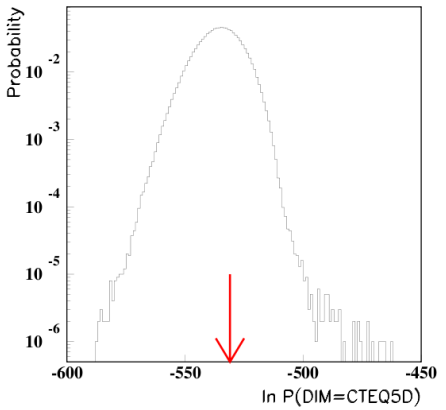

P-value is calculated by integrating out the probability from the left edge till red for the given PDF

Systematic uncertainties

δ_1 Vertex rescaling

- More secondary vertex in MC. For the nominal result, a rescaling is applied for both N_c and N_{bg}. For systematic, this was only applied on N_{bg}.

δ_2 EW charm fraction

- QCD contribution to MC charm signal is taken as a systematic uncertainty.

δ_3 LF background

- Uncertainty associated with remaining LF background was estimated by varying N_{bg} by $\pm 30\%$.

δ_4 CC DIS selection

- Taken from previous ZEUS analysis. (arXiv:1008.3493)

δ_5 Jet energy scale

- Uncertainty associated with calorimeter is ~3%. Measurement was repeated with E_T cut varied by ~3% in the MC.

δ_6 Luminosity (**Not included**)

- Uncertainty in ZEUS luminosity measurement is ~2%.

δ_7 Signal extraction method & secvtx selection (**Not included**)

- This could only be tested with the low statistics available at the cross section stage and was not included in the final number. It could be as large as $\pm 6\ pb$.

Sources	$\delta\sigma^{+}_{c^{EW}}\ (pb)$	$\delta\sigma^{-}_{c^{EW}}\ (pb)$
Rescaling	-1.2	$+0.9$
QCD charm fraction	-0.6	-1.1
LF background	± 0.1	± 0.3
DIS selection	± 0.2	± 0.1
Calorimeter	± 0.0	± 0.1
Total	$+0.2$	$+1.0$
	-1.3	-1.2

- In MC, $\sigma_{c^{EW}} \sim 9\ pb$

Estimation of visible EW and QCD part of charm cross-section using Ariadne

e^+p	MC Contribution (%)			
	$d \to c$	$s \to c$	$\bar{c} \to \bar{s}(\bar{d})$	$g \to c\bar{c}$
$\sigma^{MC}_{c,vis} + \sigma(g \to c\bar{c})$	9	45	40	6
$\sigma^{MC}_{cEW} + \sigma(g \to c\bar{c})$	7	31	58	4

e^-p	MC Contribution (%)			
	$\bar{d} \to \bar{c}$	$\bar{s} \to \bar{c}$	$c \to s(d)$	$g \to c\bar{c}$
$\sigma^{MC}_{c,vis} + \sigma(g \to c\bar{c})$	3	45	40	12
$\sigma^{MC}_{cEW} + \sigma(g \to c\bar{c})$	2	31	57	10